Biophysical Chemistry 11 (1980) 447–459

NON-LINEAR DIELECTRIC PROPERTIES OF NERVE MEMBRANES

Shiro TAKASHIMA
Department of Bioengineering D2, University of Pennsylvania, Philadelphia, Pennsylvania 19104, USA

The unique feature of the measurement of membrane capacitance and conductance of nerve axons is the facts that these measurements must be carried out in the presence of a bias potential (−60 mV) across the membrane and also that measurements are performed in the presence of time dependent and non-linear currents. The bias potential creates an electrical field of 80 kV/cm in the membrane which produces a highly ordered structure at the resting state. Because of this, the AC field which is used for capacitance and conductance measurements should be considered a perturbation of the ordered structure rather than the force causing a transition from a random distribution to a polarized state. If the bias potential is removed by depolarization of the membrane, the ionic permeabilities of the membrane increases and Na and K ions will flow across it. Therefore, measurements of capacitance and conductance of depolarized membranes will be carried out in the presence of these ionic currents. First of all, K^+ current is known to create an inductive reactance. Also Na current is believed, although still uncertain, to produce a capacitance component. Therefore, these reactances must be differentiated from the real membrane capacitance due to the dielectric properties of the components of the membrane. In order to do so, it is desirable to conduct dielectric measurements in the absence of ionic currents after application of appropriate toxins.

1. Introduction

Electrical properties of biological membranes have been studied by many investigators and a number of reviews are available [1–4]. Of various electrical properties, this paper concerns only admittance or impedance characteristics of membranes. In general, biological membranes can be divided into two groups. The one is passive membranes and the other, excitable membranes. Although passive and excitable membranes share to some extent similar electrical properties, there are certain fundamental differences between them. This paper excludes discussions on passive membranes and concentrates only on membranes of nerve axons.

Often, biological cells are very small and we cannot insert electrodes in these cells to measure the electrical properties such as conductances and capacitance of the membrane and cytoplasm directly. Under these circumstances, we have to use a pair of large metal electrodes placed in the suspension of biological cells [1,5,6]. Electrical properties of cell membrane and cytoplasm can be deduced mathematically from measured capacitance and conductance of cell suspensions using appropriate mixture formulae. However, in order to deduce desired electrical properties of the cell, one has to perform extensive mathematical manipulations often using simplifying assumptions. Therefore, the resolution of these techniques can be less than satisfactory for detecting small or even moderate changes in capacitance and conductance under different conditions. Also having to deal with many parameters simultaneously, it is difficult to find a unique set of electrical parameters for the cells under study.

If cells are somewhat larger, it is possible to impale them with glass microelectrodes [4,7]. These microelectrodes have a tip diameter of one micron or less and have been used primarily for the measurement of membrane potentials of various biological cells. However, these electrodes have a very large tip impedance of 10 Mohms or more. This fact made these electrodes unsuitable for impedance measurements for conventional dielectric measurements using AC impedance or admittance bridges. However, it is possible to use two microelectrodes in a cell, one of them for current injection and the other for potential measurement in order to calculate the transfer function and deduce capacitances and conductances from them. This technique has been successfully used by Falk and Fatt [8,9] and also by Eisenberg et al. [10] with single muscle fibers and produced valuable information about the structure of muscle membrane and tubular systems.

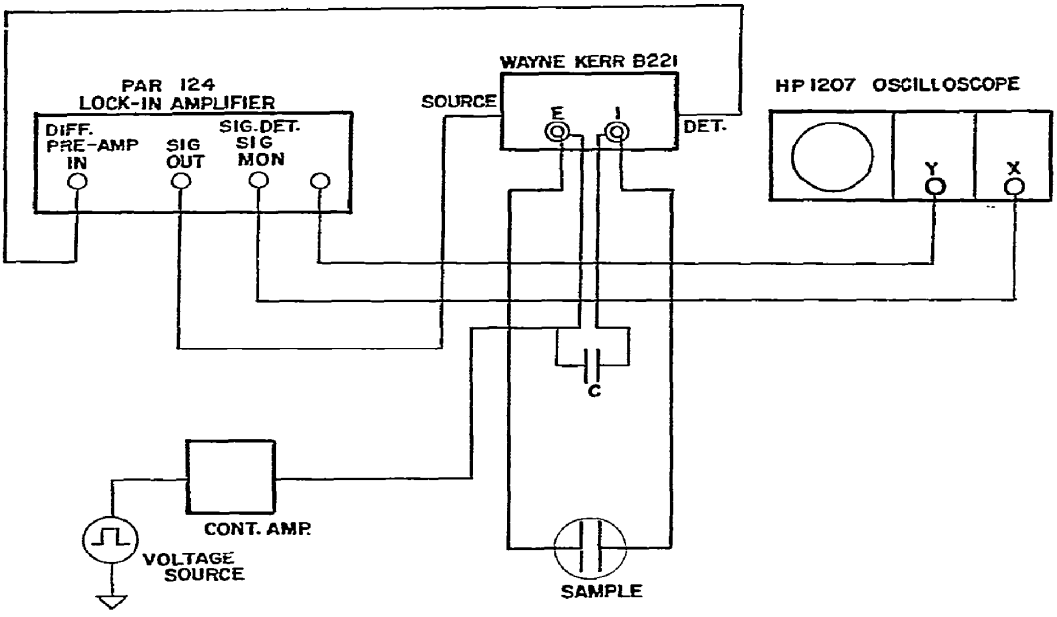

Fig. 1. Schematic diagram of measuring system.

Nerves are elongated thin cylindrical cells which are surrounded by an excitable membrane having a thickness of 70–80 Å. The diameters of nerves range from 25 to several hundred microns depending on the source of these preparations. Usually, nerves are covered with an insulator called myelin which are interrupted by active regions (Node of Ranvier). These myelinated nerves are small having a diameter of only 20–25 μm. They are too small to insert electrodes internally and we have to use special electrode arrangements, i.e., air, vaseline or sucrose gap methods [11,12]. Fortunately some sea animals such as squid or lobster have extraordinarily large nerve axons with diameters ranging from 100 to 700 μm. With these nerves we can insert internal axial electrodes from one end to the other. This arrangement enables us to measure electrical properties directly across the membrane. This is the method which has been used to investigate the electrical admittance characteristics of nerve membranes and I would like to describe the technique in some detail before the discussion of the results obtained with this sytem.

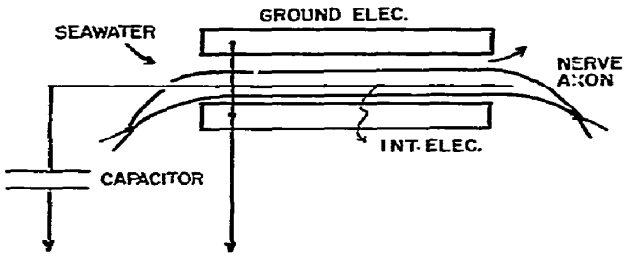

Fig. 2. Internal electrode arrangement for C_m and G_m measurements of nerve axons. A large capacitor is placed in series with the sample to block the DC shunt.

2. Method

Measurements of capacitance and conductance of nerve membranes are performed using the system shown in fig. 1. For these measurements, an admittance bridge Wayne–Kerr B221 has been used in our laboratory with a PAR 124 lock-in amplifier as a signal generator and null detector. The frequency range of this system covers between 100 Hz and 20 kHz. The electrode arrangement used for squid axons is depicted in fig. 2. Internal electrodes are a Pt-Ir wire with a diameter of 75 μm and the depth of insertion is usually 25 mm. The ground electrodes are Pt plates which are pushed against the outer wall of nerve axons. This arrangement enables us to

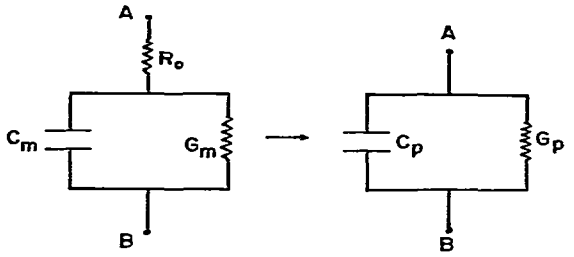

Fig. 3. Equivalent circuits of membrane admittance having a series resistance R_0. C_p and G_p are measured admittances.

measure the capacitance and conductance across the membrane unambiguously. If external electrodes are used, only certain fraction of the current would penetrate the membrane and a large fraction would go around the nerve axon thus creating a tangential component. Internal electrode arrangements are more straightforward and mathematical analyses are simpler. However, even this arrangement has several technical problems which produce systematic errors in measured capacitances and conductances.

2.1. Error due to series resistance

As illustrated in fig. 2, the space between axon membrane and electrodes is filled with seawater, axoplasm and Schwann cells. The equivalent circuit of this system is shown in fig. 3 which consists of a series resistance (R_0) and membrane admittance (C_m and G_m). R_0 represents resistances of seawater, axoplasm and Schwann cells. The capacitance and conductance measured with the electrode arrangement shown in fig. 2 actually represent the admittance between the points A and B including R_0, C_m and R_m. Analysis of this circuit readily indicates that measured capacitance and conductance are given by the following equations [13]

$$C_p = \frac{CR^2/(R_0+R)^2}{1+(\omega\tau)^2}, \quad (1)$$

$$G_p = \frac{1/(R_0+R)+\omega^2C^2R^2R_0^2/(R_0+R)^2}{1+(\omega\tau)^2}, \quad (2)$$

where

$$\tau = CR_0R/(R+R_0),\ C = C_m,\ R = 1/G_m,\ \omega = 2\pi f$$

As shown, measured capacitances and conductances

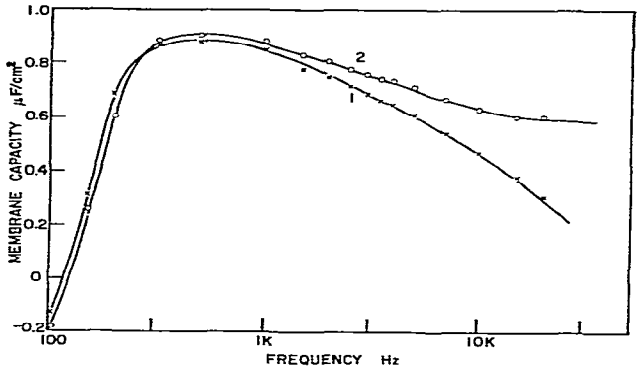

Fig. 4. Membrane capacitance before correction (curve 1) and after correction (curve 2) for series resistance.

are functions of C_m, G_m and R_0 and frequency ω. This means that as long as the value of R_0 is finite measured capacitances and conductances will be frequency dependent regardless of the nature of C_m and G_m. In order to determine the values of C_m and G_m, we have to solve eqs. (1) and (2) simultaneously. In order to do so, we must find the value of R_0 first. The value of R_0 can be determined from the conductance G_p at high frequencies where the membrane is electrically shunted. R_0 is however determined more accurately using "Impedance plots" as described in the previous publication [15]. Usually the value of series resistance is about 7–10 ohms cm^2 [14] for the electrode arrangement used in our experiments. This value is much smaller than the resistivity of resting membranes (1 kohm cm^2 or more). However, the presence of this resistance is enough to produce a false frequency dependence of measured capacitances as shown in fig. 4. In particular, during action potentials when membrane resistivity decreases, the error due to series resistance becomes even more serious.

2.2. Fringe effect of internal electrode

Inspection of fig. 2 reveals that if one sures capacitance and/or conductance using this electrode arrangement, there will be a spurious component due to the fringe effect at the tip of the internal electrode. The relative magnitude of the stray capacitance should be small if the length of the internal electrode is chosen to be very long. Takashima and Tasaki (unpublished data) found that the fringe effect amounts to 20–25% of the

total capacitance using an electrode with a length of 17 mm. Moreover, fringe capacitance is found to be dependent on frequency. The error due to stray capacitance will, therefore, create serious errors on membrane capacitance and its frequency dependence. However, experimentally, accurate determination of stray capacitance is not a trivial procedure. Use of guard electrodes turns out to be very difficult. A compromise is to change the length of electrodes and interpolate the measured capacitances to zero length. This method is cumbersome and not practical. Nevertheless, it is advisable to use an internal electrode as long as possible to reduce the relative magnitude of stray capacitance. We use an electrode of 25 mm and insert it all the way from one end to the other. Although this technique does not eliminate the fringe effect completely, this seems to be the only acceptable experimental method at present.

Recently, Schwan (personal communication) based on the transmission line theory calculated the fringe effect as shown in eqs. (3) and (4)

$$G_s^2 = (G/2R)\{1 + (1 + \omega C)^2/G)^{1/2}\}, \quad (3)$$

$$(\omega C_s)^2 = (G/2R)\{-1 + (1 + (\omega C)^2)^{1/2}\}, \quad (4)$$

where C_s and G_s are stray capacitance and conductance, C and G are measured membrane capacitance and conductance at given frequencies. R is resistance of axoplasm. Although the value of fringe capacitance calculated with this equation tends to be too large compared with experimental results, nevertheless, they seem to predict the behavior of fringe capacitance and conductance including their frequency dependence reasonably correctly.

2.3. Electrode polarization

One of the major difficulties for dielectric measurements with aqueous solutions is the error caused by electrode polarization [5]. This effect usually produces a large capacitance at low frequencies and at times it becomes almost impossible to determine the low frequency limiting value of dielectric constant. Resting nerve membranes have a resistivity of 1 kohm cm^2 and the effect of electrode polarization is generally negligible as shown in fig. 4. However, during excitation, membrane resistivity decreases considerably and under these circumstances the error due to electrode polarization must be analyzed carefully. However, we have not detected the presence of electrode polarization even during depolarizations of membranes and during the action potential.

3. Results and analyses

3.1. Membrane capacitance at resting state

As well known, the electrical potential of external solution is higher than that of the interior of nerve axon by about 60 mV. Since the thickness of nerve membranes is 70–80 Å, the field strength existing in the membrane amounts to almost 80 000 V/cm. The field of this magnitude is usually sufficient to produce a highly polarized state in the membrane. Not only lipid molecules but also protein molecules in the membrane are likely to be in an ordered state. For the measurement of membrane capacitance, we perturb ordered molecules with a small AC field. Since we use an AC field with an amplitude of 1–2 mV for these measurements, the field strength of AC signals in the membrane will be about 1000 V/cm. With this perturbation, proteins and/or lipid molecules will undergo small shifts from the resting equilibrium states. One of the results of membrane capacitance measurements is shown in fig. 4 [15].

First of all, measured capacitances decrease sharply with increasing frequencies as predicted by eq. (1). After the correction for series resistance however, we obtain the true membrane capacitance. As shown in this figure, membrane capacitance of squid axon seems to be frequency dependent decreasing from 1 $\mu F/cm^2$ to 0.6 $\mu F/cm^2$ between 200 Hz and 20 kHz. Although the frequency dependence of membrane capacitance appears real, certain portions of it may be due to the fringe capacitance discussed before and there is still some ambiguity concerning it. If it is real, the small frequency dependence of the capacitance may be indicative of the presence of certain freedom of membrane components even in the presence of an intense field of 80 kV/cm. The membrane capacitance is independent of the amplitude of AC signals within ±5 mV indicating that resting membrane behaves as a linear system within this range. However, fig. 4 indicates the presence of anomalous inductive component [1,16] and as discussed later, this behavior is attributed to time dependent and non-linear K^+ current. In this sense, even resting membranes show a non-linear behavior.

As the frequency of AC signals increases above 10 kHz, membrane capacitance approaches asymptotically a limiting value of 0.6 $\mu F/cm^2$. As mentioned later, this value is very similar to the capacitance of artificial lipid bilayer membranes [17,18]. Thus, it is reasonable to attribute this part of the membrane capacitance to lipid molecules whereas the low frequency capacitance may be attributed to protein molecules which are, according to the model by Singer and Nicolson [19], partially or totally embedded in the membrane.

3.2. Voltage dependence of membrane capacitance

Years ago, Cole and Curtis observed that membrane capacitance of squid axon is independent of membrane potential whereas membrane conductance increased enormously during the action potential [20,21]. Since ionic channels undergo a transition from a closed state to an open state during the action potential, the conductance increase can be easily explained at least qualitatively. While the conductance of resting nerves represents the resistivity of membrane bulk including closed ionic channels, those of excited nerves represent the conductance of open ionic channels. The constancy of membrane capacitance, on the other hand, indicates that excitation does not produce an extensive change in the membrane configuration. Namely, opening of ionic channels is a localized event and does not require conformation changes of membrane components.

However, recently, several groups observed a capacitive current associated with the opening of sodium channels [22–25]. This means that there are certain groups of molecules with a dipole moment in or near sodium channels and that these dipolar molecules reorient themselves when the membrane is depolarized leading to the opening of ionic channels. Therefore, according to these new results, excitation of nerve membrane must involve movements of dipolar particles which must manifest itself as a capacitance increase. The measurement of displacement current or "gating current" is usually performed using time domain techniques. If a gating current is detected in the time domain measurement, frequency domain measurements must also detect an increase in capacitance. Since Cole and Curtis already concluded some years ago that membrane capacitance remains constant during depolarizations or action potentials, the observation of gating current is incompatible with the classical experiments by Cole et al. According to the calculation by Taylor and Bezanilla, the expected capacitance change if measured in the frequency domain, will be 0.4 $\mu F/cm^2$. A capacitance change of this magnitude cannot be overlooked by any dielectric measurements.

Table 1
Membrane capacitances at rest and at the peak of normal action potential

Frequency (kHz)	C_m (rest) $\mu F/cm^2$		C_m (excited) $\mu F/cm^2$	
	uncorrected	corrected	uncorrected	corrected
2	0.760	0.817	0.766	0.991
3	0.687	0.766	0.690	0.971
5	0.609	0.720	0.554	0.868
10	0.469	0.615	0.388	0.701

Some years ago, Schwan [27] discussed Cole's conclusion pointing out that Cole et al's measurements were carried out at high frequencies and that if the frequency was extended to lower regions, they would have observed a capacitance change as well as the conductance increase. In order to investigate the voltage dependence of membrane capacitance and conductance, there are two ways to do so. The one is to apply square pulses under current clamp conditions and the other is to trigger action potentials by short pulses and measure the admittances at the peak of the impulses. Although we carried out both measurements [13,28], I would like to discuss only the results of transient measurements during the action potentials. First of all, the duration of ordinary action potential is only 1.5 ms and the short duration makes the transient measurement exceedingly difficult at low frequencies. While the measurements by Cole and Curtis were limited to 20 kHz, we managed to measure capacitances and conductances during action potentials at as low as 2 kHz. We found, as shown in tabie 1, that measured capacitances remain constant at the peak of the action potential as claimed by Cole and Curtis. Therefore, it became clear that merely extending the measurements to low frequencies will not reveal capacitance increases as predicted by Schwan. However, it must be emphasized that table 1 tabulates only measured capacitances without the correction for series resistances. From eq. (1), we can easily derive the following equation at low frequencies where $\omega \to 0$

$$C_p = \frac{C_m}{(1 + R_0/R_m)^2}. \quad (5)$$

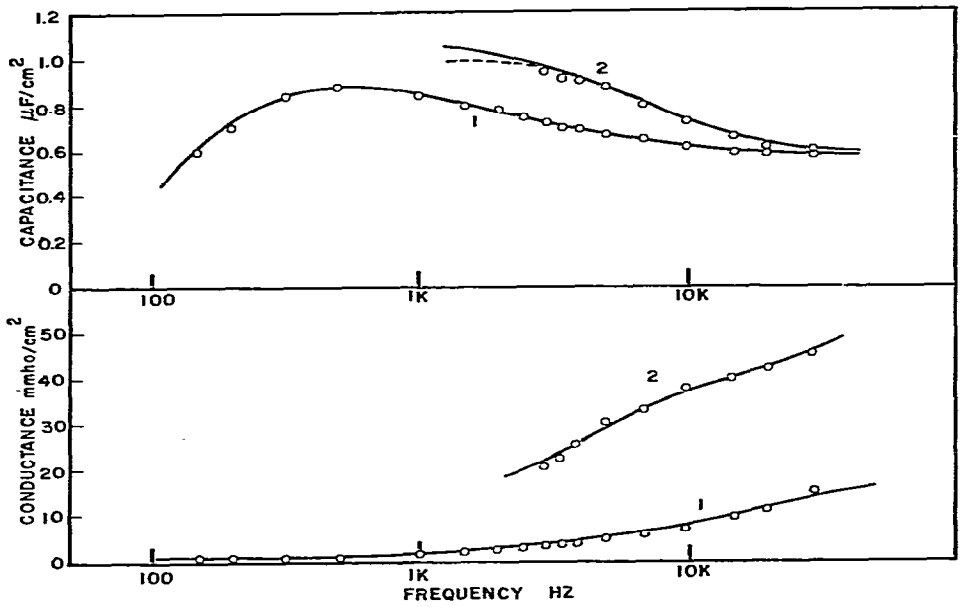

Fig. 5. (a) Membrane capacitances at rest (curve 1) and at the peak of normal action potential (curve 2). Dashed curve indicates possible inductive behavior. (b) Membrane conductances at rest (curve 1) and at the peak of normal action potential (curve 2).

In this equation, the ratio R_0/R_m is very small at the resting state (5–10 ohms cm^2 for R_0 and 1–5 kohms cm^2 for R_m). Therefore, the quantity in the brackets is nearly unity for resting membranes and hence measured capacitance is almost identical to the real membrane capacitance at low frequencies where eq. (5) holds. However, during action potentials membrane resistance decreases considerably and R_m becomes almost comparable to R_0. Under these circumstances, the quantity $(1+R_0/R_m)^2$ becomes larger than unity. Therefore, measured capacitances C_p during the action potential are smaller than membrane capacitance C_m at all frequencies. Close examinations of Cole's data reveal that the value of series resistances in their electrode arrangement is much larger than ours. Thus, it became apparent that the constancy of membrane capacitance or its slight decrease may have been due to the presence of series resistances.

We made an extensive investigation on the voltage dependence of membrane capacitance of squid axons. In these experiments, an admittance bridge is balanced to the resting membrane and capacitance and conductance are recorded. In order to trigger the action potential, short electrical pulses are applied to the axon through the neutral lead of isolation transformer of the bridge. This method enables us to elicit space clamped action potentials uniformly. By displaying both the action potential and admittance change on an oscilloscope, we can confirm that they are almost in phase with each other and that the admittance change is indeed due to the action potential. We then re-adjust the capacitance and conductance knobs manually during recurring action potentials until we rebalance the bridge to the excited membrane. The same procedure is repeated at frequencies between 2 and 20 kHz. Since the duration of the normal action potential is only 1.5 ms, transient measurements are restricted above 2 kHz. In spite of this limitation, fig. 5 clearly indicates an enormous increase in conductance as observed by Cole et al. and also demonstrates a moderate increase in membrane capacitance from 1 μF/cm^2 to 1.15 μF/cm^2 contrary to Cole's conclusion. As it is obvious from this figure, the frequency range of these measurements is too limited to establish the low frequency end of the dispersion curve. Transient measurements with normal action potentials below 2 kHz is prohibitingly difficult. In addition to this, a careful examination will reveal that the slope of the dispersion curve is actually steeper than the Debye

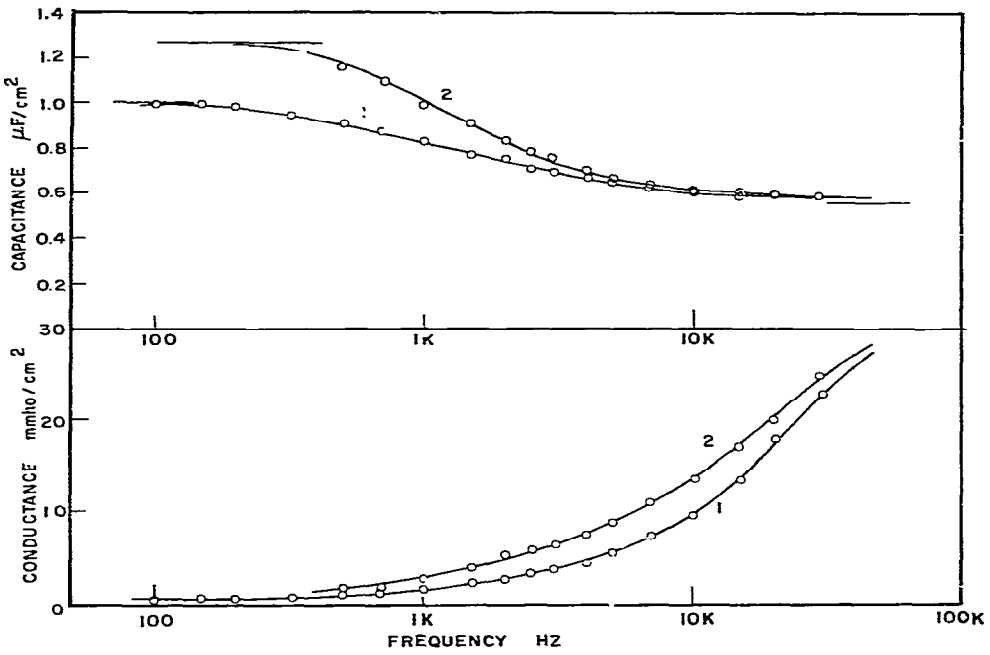

Fig. 6. Membrane capacitances with 15 mM TEA in the axon. Curve 1, at rest and curve 2 at the peak of long action potential. Note the absence of inductive behavior. Horizontal lines are low and high frequency limiting capacitances calculated from the Cole and Cole plots (ref. [32]). The lower diagram shows conductances with TEA. Curve 1, resting state and curve 2, during the long action potential.

theory of one time constant, a physically impossible phenomenon. Reflecting this, the imaginary part is considerably larger than the half amplitude of the dispersion, i.e., $C''_m > (C_0 - C_\infty)/2$. These observations indicate that the full dispersion curve is truncated by the presence of a component as shown by a dashed curve. This component, i.e., inductive component, is present even in the resting membrane (see fig. 5). As discussed later, the inductive component is, according to Cole, due to K^+ current. Since K^+ current increases during the action potential, it is quite reasonable to assume that the inductive element also increases and begins to offset capacitance increases. Therefore, the curve shown in fig. 5 is the net result of these two changes, i.e., increases in capacitance and inductance in opposite directions. Thus the real dispersion curve should be the one indicated by the solid curve. Under these circumstances, it is desirable to eliminate the inductive component by blocking the potassium current in order to study the behavior of the capacitive element unequivocally. It is well known that quarternary ammonium salts such as tetra-ethyl ammonium chloride (TEA) selectively block the potassium current if it is added in the axoplasm using internal perfusion techniques [29, 30]. Using these compounds, we can eliminate K^+ current without affecting the sodium current and thus we can eliminate the inductive element without affecting the capacitive component. Also it is well known that blocking the potassium current prolongs the action potential [30,31]. Therefore, we achieve elimination of inductive element and prolong action potential by blocking K^+ current. Because of the latter, we are able to extend the frequency of admittance measurements during the action potential down to 500 Hz or even lower. As clearly seen from curve 1 in fig. 6a, the inductive component which interfered with the measurement of capacitance during the normal action potential is eliminated by this procedure. Curve 2 in the same figure shows the capacitance at the peak of the long action potential at various frequencies. As seen, membrane capacitance increases from 1 μF/cm^2 to 1.25 μF/cm^2. This increase is somewhat smaller than the expected value of 1.4 μF/cm^2. This may be due to the fact that blockage of K^+ current decreases the sodium current to

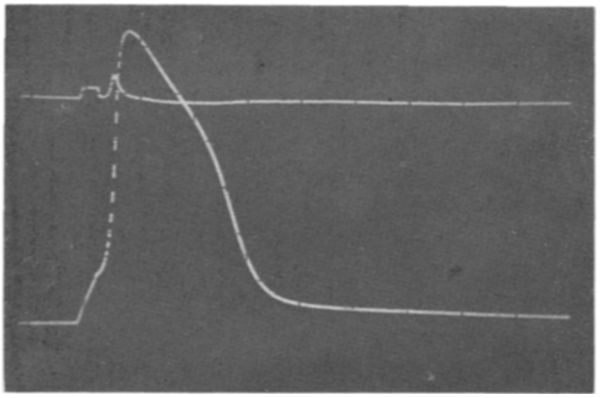

Fig. 7. Prolonged action potential in the presence of 15 mM TEA. Lower trace is potential change. Upper trace shows the current diagram. The first spike is due to stimulus and the second is due to capacitive current. Both are outward currents.

some extent. Since potassium channels are blocked by TEA, the capacitance and conductance changes observed are clearly due to the sodium channels alone. It is important to emphasize that the conductance increase observed during the normal action potential is almost completely eliminated in this case (see fig. 6b). Only AC conductance which is essentially due to orientation of dipolar molecules was found to increase slightly reflecting the capacitance increase mentioned above. This observation is quite puzzling because it has been well accepted that sodium ions flow through the membrane inwardly during the early stage of the action potential producing a large increase in DC conductance. Our results indicate that 1) DC conductance increase observed during the normal action potential is due to K channels alone and 2) the charge movement due to the sodium current is bound within the membrane rather than flowing through it. Fig. 7 shows the net current observed during the long action potential in the absence of K^+ current. Contrary to our expextation that a large sodium inward current would be observed because of the absence of K^+ current which normally compensates the Na^+ current, we actually observed a vanishingly small net current. These two observations indicate puzzling features of the sodium current in the nerve membrane treated with TEA.

Analyses of dispersion curves shown in fig. 6a demonstrate difference in their slopes. Namely the slope of the dispersion curve during the action potential is steeper than that of resting membranes. Generally, dispersion curves can be fitted to the following equation proposed by Cole and Cole [32] rather than the Debye equation [33].

$$C_0 - C_\infty = (C_0 - C_\infty) \times \frac{1 + (f/f_c)^n \cos n(\pi/2)}{1 + (f/f_c)^n \cos n(\pi/2) + (f/f_c)^{2n}}, \qquad (6)$$

where f_c is relaxation frequency, C_0 and C_∞ are low and high frequency limiting capacitance, and $n = 1 - \alpha$ (α = distribution parameter for relaxation times ranging from 0 to 1). Using this equation, we can calculate theoretical curves assuming a proper value for the parameter n or α. The solid curves drawn through observed points are obtained assuming $\alpha = 0.21$ for resting membranes and 0.03 for excited membranes. Namely, at rest, the relaxation of membrane components is characterized by several time constants while that of excited membrane by only one time constant.

The results presented above clearly demonstrate that capacitance of nerve membrane increases during the action potential contrary to the conclusion by Cole and Curtis. Our observations seem to solve the gap existing between Cole's conclusion and recent observations of gating currents. However, there are still some important unsettled problems concerning the gating current and capacitive increases during activity. This discussion is beyond the scope of this article and references are given [34,26]. The nature of the capacitance increase is still unknown. In general, there may be two possible mechanisms. Namely, change in the membrane permittivity due to the change in the conformation of channel particles or capacitance changes due to the sodium current itself. Thickness changes of the membrane can be ruled out because the high frequency capacity which represents the capacity of lipid bilayers remains constant during the action potential. Before we discuss the mechanism, I would like to describe a problem of inductive behavior of the nerve membrane.

3.3. Inductive reactance

As clearly shown in fig. 4 and fig. 5, frequency dependence of the capacitance of nerve membrane is anomalous at low frequencies in that capacitance diminishes with decreasing frequencies. This behavior cannot be explained unless nerve membranes have an inductive element in addition to a capacitive component. It has been dis-

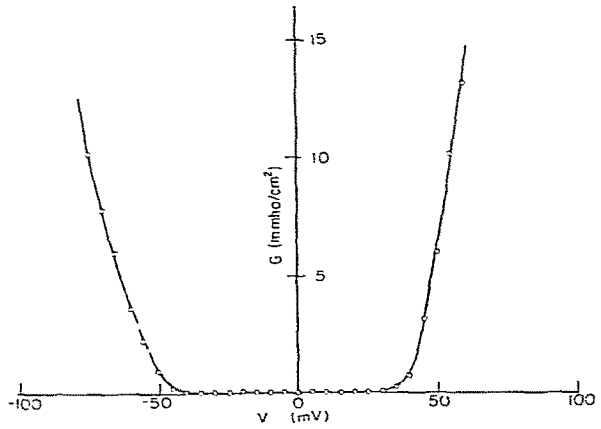

Fig. 8. Conductances versus membrane potential of lipid bilayer membrane (egg lecithin in hexadecase) in the presence of 10^{-7} mol of alamethicin. Frequency 500 Hz.

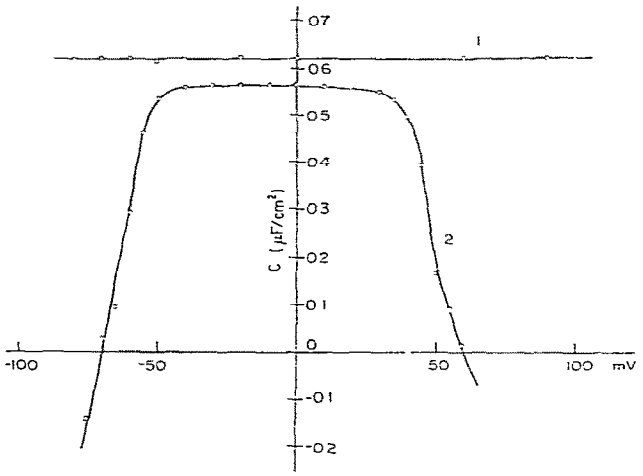

Fig. 9. Capacitance versus membrane potential of egg lecithin membrane in the presence of 10^{-7} mol alamethicin (curve 2). Curve 1 is plain membrane showing voltage independence of membrane capacitance. Note that capacitances dip into negative values in curve 2 with large hyper- and depolarizations. Frequency 500 Hz.

cussed that the inductive element is not due to the structure of the membrane but it may be due to time dependent non-linear current [1,35,36]. In particular, K^+ current, which is not insignificant even at the resting state has been considered responsible for the inductive behavior. K^+ flux produces a slow current with a sigmoidal rising phase and is considered non-linear with applied voltages. In order to confirm this argument, we attempted to simulate the inductive behavior using a model membrane which consists of egg lecithin and a solvent hexadecase. In general, lipid bilayer membranes have an enormous resistivity and do not permit ion fluxes through them. However, it is well known that certain peptides such as gramicidin, varinomycin and alamethicin when they are added in the bating solution, increase the permeabilities of these membranes [37–39]. Of particular interest to us is alamethicin. This compound produces a slow rising and non-linear current which is similar to K^+ current in nerve membranes. This compound is, therefore, almost ideal for our purpose to simulate the inductive behavior. The procedures of forming artificial bilayer membranes are well documented by Mueller and Rudin [40] and we followed their method. Membranes are formed in an aperture having a diameter of 0.5 mm and membrane capacitance is measured using the method described above with two electrodes placed on both sides of the aperture. First of all, the capacitance, as pointed out before, are very close to the high frequency capacitance of nerve membrane. It was found by Takashima and Schwan [41] that the capacitance of lipid bilayer membranes is frequency independent within the experimental error, a behavior considerably different from the nerve membrane. Moreover, applied voltages do not have any effects on membrane capacitance and resistance even at ±250 mV. In other words, plain bilayer membranes behave like a solid dielectric wall without any relaxation phenomena. When alamethicin is added to the membrane (0.1–1 μM), the resistivity remains almost the same if no external pulses are applied. However, if the membrane is perturbed by electrical pulses, large time dependent currents can be detected. Conductances and capacitances are measured in the presence of these currents using the transient bridge method discussed above. This procedure is repeated for various potentials and frequencies. Fig. 8 and fig. 9 illustrate conductance and capacitance readings obtained during long pulses (duration 50–100 ms) at 0.5 kHz. Similar to the nerve membrane, we observed enormous increases in conductance with applied potentials. The fact that the curve is asymmetric on both sides of the y axis is because alamethicin is added only on one side. On the other hand, capacitance was observed to decrease markedly with ap-

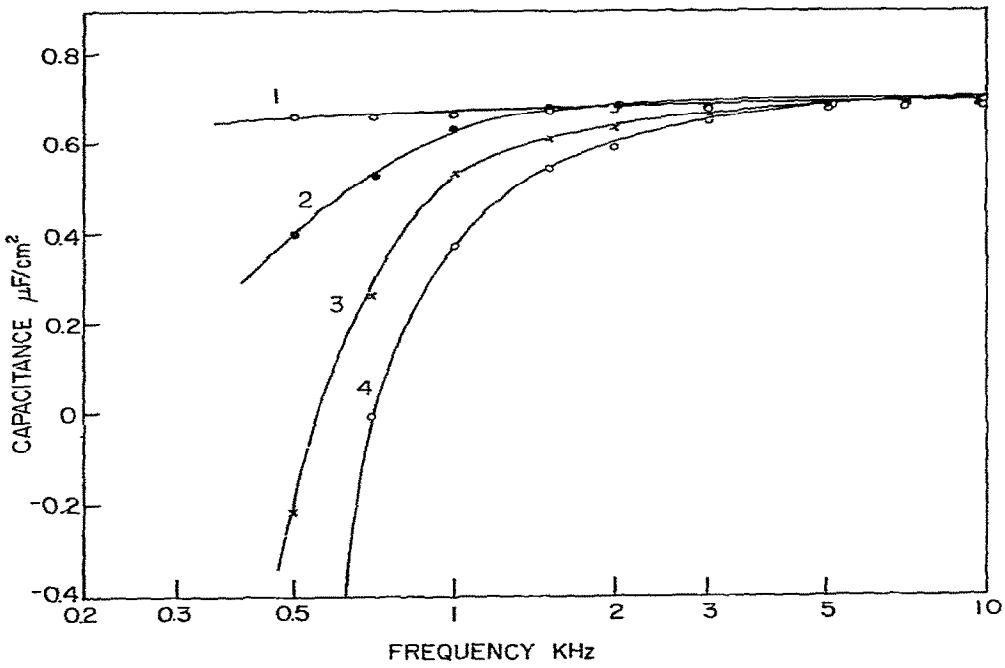

Fig. 10. Anomalous frequency dependence of measured capacitances of egg lecithin membranes with 40 mV (curve 1), 45 mV (curve 2), 50 mV (curve 3) and 65 mV (curve 4) depolarizations. Duration of pulses 100 ms.

plied potentials and often turns into negative values with large depolarizing and hyperpolarizing potentials. Fig. 10 shows the anomalous dispersion curve obtained at various frequencies for a fixed depolarization of +80 mV. This figure should be compared with fig. 4 shown before. These two curves are quite similar in that they both exhibit an anomalous inductive dispersion at low frequencies although their behavior above 1 kHz are different. This observation clearly demonstrates that the anomalous inductive behavior observed first by Cole and Curtis with nerve axons and has been puzzling investigators for many years can be simulated easily using model membranes. In other words, the inductive behavior is not necessarily unique to nerve membranes but can be produced in other membranes as long as we can create time dependent non-linear currents. Also the inductive behavior should be observed widely in other biological membranes such as muscle membranes where non-linear ionic currents are present.

3.4. Mechanisms of capacitance and inductance changes

As has been discussed, the inductive behavior in biological and artificial membranes can be produced by non-linear time dependent currents. In nerve membranes, it is believed that K^+ current is responsible for the inductive behavior. Although Na current is also non-linear and time dependent, Na current is believed to produce a capacitive component. The time dependence and non-linear behavior of sodium and potassium currents are well documented by the Hodgkin–Huxley equation [42]. If one perturbs the Hodgkin–Huxley equation with a small depolarizing pulse, a small amount of current δI will flow through the membrane. For these small depolarizations one can linearize the Hodgkin–Huxley equation by retaining the first term of Taylor series. The Fourier Transform of the linearized Hodgkin–Huxley equation produces a frequency domain expression for complex conductivities for sodium and potessium components as shown by eq. (8) [43].

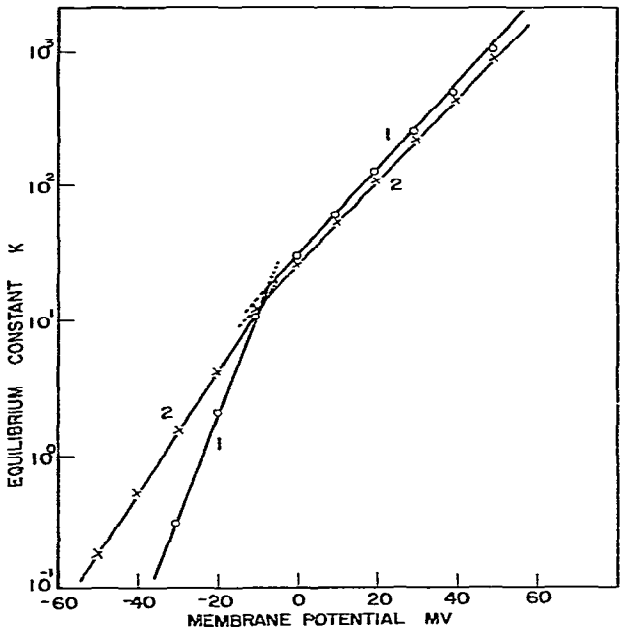

Fig. 11. Voltage dependence of equilibrium constants calculated from $K = \alpha_m/\beta_m$. Curve 1 is obtained from the best curve-fitting to the recorded Na current. Curve 2 is calculated with the Hodgkin–Huxley equation.

$$Y(\mathrm{Im}) = \mathrm{j}\omega \times \left\{ c - \frac{g_n \tau_n}{1+(\omega\tau_n)^2} - \frac{g_m \tau_m}{1+(\omega\tau_m)^2} - \frac{g_h \tau_h}{1+(\omega\tau_h)^2} \right\} \quad (8)$$

where parameters g_n, g_m and g_h are given by eqs. (9), (10) and (11)

$$g_n = 4\bar{g}_K n^4 (V - V_K)(\partial/\partial V)(\ln n)\,, \quad (9)$$

$$g_m = 3\bar{g}_{Na} m^3 h (V - V_{Na})(\partial/\partial V)(\ln m)\,, \quad (10)$$

$$g_h = \bar{g}_{Na} m^3 h (V - V_{Na})(\partial/\partial V)(\ln h)\,, \quad (11)$$

where n, m and h are parameters defined by Hodgkin and Huxley. It must be noted that these are expressions for frequency dependent capacitances and inductances and that the term for K^+ current is negative whereas that for Na^+ current is positive for membrane potentials between −70 and +56 mV (V_K is about −70 mV and V_{Na} is +56 mV). Therefore in this range of membrane potential, sodium current produces a capacitive component while K^+ current creates an inductive element.

As discussed in the foregoing, we can simulate the inductive behavior using model membranes. For these systems, the membrane potential is zero and the linearized Hodgkin–Huxley equation is generalized to be:

$$Y(\mathrm{Im}) = -\bar{g}_n n^{k-1} \frac{k(\partial n/\partial V)}{1+(\omega\tau_n)^2}(V - V_0)\,. \quad (12)$$

where we can assume that $V_0 = 0$ and the parameter k is believed to be near 6.0 for alamethicin. This equation produces a negative capacitance for positive voltages, i.e., pulses raising the potential of alamethicin side. . Thus, we can simulate the inductive behavior. In order to simulate the capacitive behavior, we have to apply negative potentials, i.e., lowering the potential of the alamethicin side. However, this experiment turned out to be difficult because it is almost impossible to create a sharp alamethicin concentration gradient due to leakage. As shown in fig. 9, hyperpolarizing pulses also produce inductive element to confirm this argument.

As has been discussed, the origin of inductive component is most likely to be due to time dependent ionic current. However, the origin of capacitive component which is due to sodium channels is still debated. Hodgkin and Huxley [42] postulated years ago, that opening of ionic channels may be due to orientation of dipolar particles or due to some kind of chemical reactions. The first concept led to the attempts to find "gating current". The latter can be reinterpreted using a recent concept of dielectric relaxation due to chemical reactions. Bergman, De Maeyer and Eigen [44] proposed that if a chemical reaction such as shown by eq. (12) creates a product possessing a dipole moment which is different from that of the reactant A, the chemical relaxation can produce a frequency dependent dielectric constant. The equilibrium constant K of the reaction will be a field dependent quantity and the difference in the dipole moment between compounds A and B can be calculated by eq. (13), if temperature and pressure are constant.

$$\mathrm{A} \underset{k_2}{\overset{k_1}{\rightleftarrows}} \mathrm{B}\,, \quad (12)$$

$$\Delta\mu = RT\,\partial \ln K/\partial E\,. \quad (13)$$

If we apply this concept to ionic channels, the capacitance change or displacement current may be due to conformation changes of gating particles such as dissociation or association of subunits [45]. Since it is diffi-

cult to measure the rate of the conformation change of gating particles directly, we measure the rate of sodium currents with various depolarizations assuming that gate opening determines the rate of sodium current. These rate constants, according to the Hodgkin–Huxley formalism, are designated by α_m and β_m. The procedure is first to calculate theoretically the values of α_m and β_m using the Hodgkin–Huxley equation for given depolarizations for 6.3°C. These values are adjusted to the experimental temperature assuming the Q_{10} value to be 3. Finally another adjustments are made so that we can obtain the best curve fits with observed curves. Equilibrium constants are easily calculated from rate constants and they are plotted against the field strength or membrane potential. One of these plots is shown in fig. 11 [46]. According to eq. (13), the plot of $\ln K$ against the field strength should give a straight line. As seen in fig. 11, the plot consists of two linear portions. From the slope of these straight lines, we can calculate the dipole moment changes of 1000 D.U. between −60 and −20 mV and 700 D.U. between −20 mV and + 40 mV. These values are reasonably consistent with those obtained by Levitan and Palti [47]. It is interesting to note that the theoretical calculation using the Hodgkin–Huxley equation for 6.3°C also produces a similar plot having two linear portions as shown in the same figure. These observations means that opening of sodium channels proceeds in two steps. During the removal of negative bias potential, i.e., −60 mV to 0 mV, there is a large change in dipole moment whereas during the second phase, addition of positive bias potential, the dipole moment change becomes smaller. As has been discussed, the concept that opening of sodium channels being due to conformation changes of gating particles produces an interesting consequence. Use of a concept that opening of channels is due to orientation of gating particles may lead to some difficulty as pointed out by Schwarz [45]. Under these circumstances, the theory proposed by Schwarz based on the concept of chemical relaxation may deserve a serious consideration.

The author wishes to acknowledge Drs. K.S. Cole, H.P. Schwan and H.M. Fishman for their helpful discussions. The author is partially supported by a grant from ONR N00014-76-C-0642.

References

[1] K.S. Cole, Membranes, impulses and ions (University of California Press, Berkeley, Calif. 1968) Chapt. 1.
[2] H.P. Schwan, Advances in biological and medical physics, Vol. V, eds. J.H. Lawrence and C.A. Tobias (Acad. Press, 1957).
[3] R. Plonsey, Bioelectric phenomena (McGrawhill, New York, 1969).
[4] O.F. Schanne and E.R.P.-Ceretti, Impedance measurements in biological cells (Wiley-Interscience, New York, 1978).
[5] H.P. Schwan, Physical techniques in biological research, ed. W.L. Nustak, Vol. 6 (Academic Press, New York, 1963).
[6] T. Hanai, Biophysics Struct. Mechanism 1 (1975) 285.
[7] L.A. Geddes, Electrodes and the measurement of bioelectric even s (Wiley, New York, 1972).
[8] G. Falk and P. Fatt, Proc. Roy. Soc. 13 (1964) 69.
[9] G. Falk and P. Fatt, J. Physiol. 198 (1968) 627.
[10] R.S. Eisenberg, J. Gen. Physiol. 50 (1967) 1785.
[11] B. Hille, Frog neurophysiology, eds. R. Llinas and W. Precht (Springer-Verlag, Berlin-Heidelberg, 1976).
[12] F.T. Julian, J.W. Moore and D.E. Goldman, J. Gen. Physiol. 45 (1962) 1217.
[13] S. Takashima and H.P. Schwan, J. Membrane Biol. 17 (1974) 51.
[14] J.W. Moore, Physical techniques in biol. research, ed. W.L. Nustak, Vol. 6 (Acad. Press, New York, 1963).
[15] S. Takashima, J. Membrane Biol. 27 (1976) 21.
[16] K.S. Cole, J. Gen. Physiol. 25 (1941) 29.
[17] T. Hanai, D.A. Haydon and J. Taylor, Proc. Roy. Soc. A 281 (1964) 377.
[18] S. White and T.E. Thompson, Biochim. Biophys. Acta 323 (1973) 7.
[19] S.J. Singer and G.L. Nicolson, Science 175 (1972) 720.
[20] K.S. Cole and H.J. Curtis, Nature 142 (1938) 209.
[21] K.S. Cole and H.J. Curtis, J. Gen. Physiol. 22 (1939) 649.
[22] C.M. Armstrong and F. Bezanilla, Nature 242 (1973) 459.
[23] R.D. Keynes and E. Rojas, J. Physiol. 233 (1974) 393.
[24] H. Meves, J. Physiol. 243 (1974) 847.
[25] W. Nonner, E. Rojas and R. Stampfli, Pflugers Archiv Für J. Physiol. 345 (1975) 1.
[26] R.E. Taylor and F. Bezanilla, Biophys. J. 26 (1979) 338.
[27] H.P. Schwan, Second International Biophys. Congress, Vienna Austria (Paper Sy-1A) 1966.
[28] S. Takashima, Biophysical Journal 26 (1979) 133.
[29] I. Tasaki and S. Hagiwara, J. Gen. Physiol. 40 (1957) 859.
[30] C.M. Armstrong and L. Binstock, J. Gen. Physiol. 48 (1965) 859.
[31] I. Tasaki, Nerve excitation, a macromolecular approach (C.C. Thomas Publisher, Springfield, Ill. 1968).
[32] K.S. Cole and R.H. Cole, J. Chem. Phys. 9 (1941) 341.
[33] P. Debye, Polar molecules (Dover Pub., New York, 1929).
[34] S. Takashima, Biophys. J. 22 (1978) 115.

[35] H.M. Fishman, Proc. First Symp. on Testing and identification of nonlinear systems, eds. G.D. McCann and P.Z. Marmarelis (Cal. Tech. Pasadena, Calif., 1975).
[36] H.M. Fishman, D.T. Poussart and L. Moore, J. Mem. Biol. 32 (1977) 255.
[37] P. Mueller, Nature 213 (1967) 603.
[38] S.B. Hladky and D.A. Haydon, Biochim. Biophys. Acta 274 (1972) 294.
[39] G. Stark, B. Ketterer, R. Benz and P. Lauger, Biophys. J. 11 (1971) 981.
[40] P. Mueller and D.O. Rudin, Lab. Tech. in Membrane Biophys., eds. H. Passaw and R. Stampfli (Springer-Verlag, Berlin, 1969).
[41] S. Takashima and H.P. Schwan, Liquid crystals and ordered fluids, Vol. 2, eds. J.F. Johnson and R.S. Porter (Plenum Press, New York, 1974) p. 199.
[42] A.L. Hodgkin and A.F. Huxley, J. Physiol. 117 (1952) 500.
[43] W.K. Chandler, R. FitzHugh and K.S. Cole, Biophys. J. 2 (1962) 105.
[44] K. Bergman, M. Eigen and L. DeMaeyer, Berichte der Bunsengesellschaft für Phys. Chemie 67 (1963) 819.
[45] G. Schwarz, J. Membrane Biol. 43 (1978) 127.
[46] S. Takashima, R. Yantorno and R. Novack, Biochim. Biophys. Acta 469 (1977) 74.
[47] E. Levitan and Y. Palti, Biophys. J. 15 (1975) 239.